

Supporting Information

A 2D Layered Cobalt-Based Metal-Organic Framework for Photoreduction of CO₂ to Syngas with a Controllable Wide Ratio

Mei-Juan Wei,^{a#} Xian-Yan Xu,^{b#,*} Jia-Qi Song,^{a#} Mei Pan,^{a,*} and Cheng-Yong Su^{a,*}

^aMOE Laboratory of Bioinorganic and Synthetic Chemistry, Lehn Institute of Functional Materials, School of Chemistry, Sun Yat-Sen University, Guangzhou 510006, China. Email: panm@mail.sysu.edu.cn, cessey@mail.sysu.edu.cn

^bCollege of Chemistry and Civil Engineering, Shaoguan University, Shaoguan 512005, China. Email: sofiaxy@sgu.edu.cn

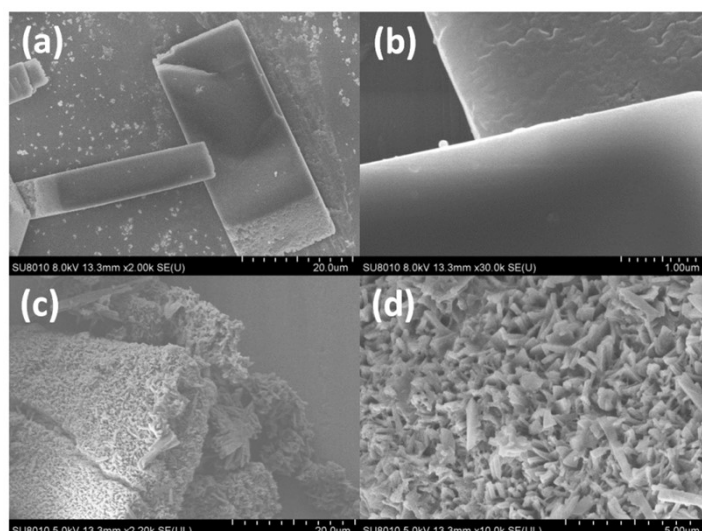


Figure S1. SEM images of Co-TBAPy before photocatalytic CO₂ reduction (a), (b); and after photocatalysis (c), (d).

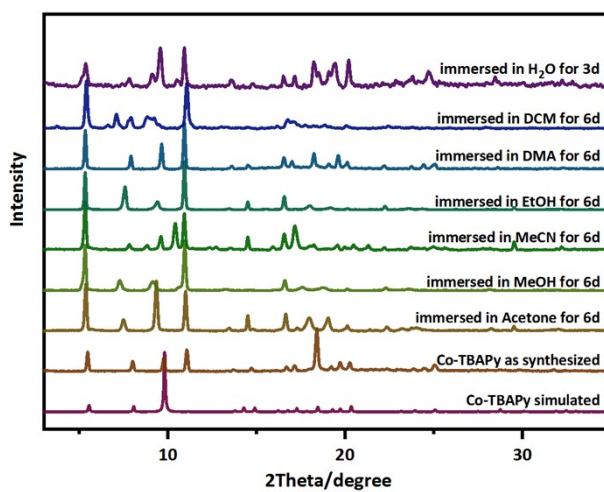


Figure S2. PXRD patterns of Co-TBAPy soaked in different solvents for a period of time.

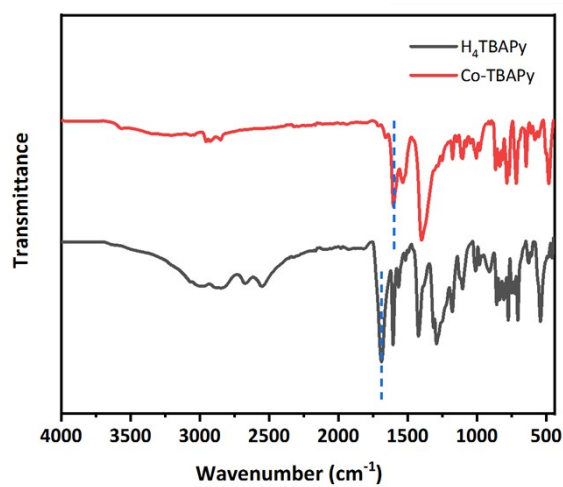


Figure S3. FT-IR spectrums of Co-TBAPy and H₄TBAPy.

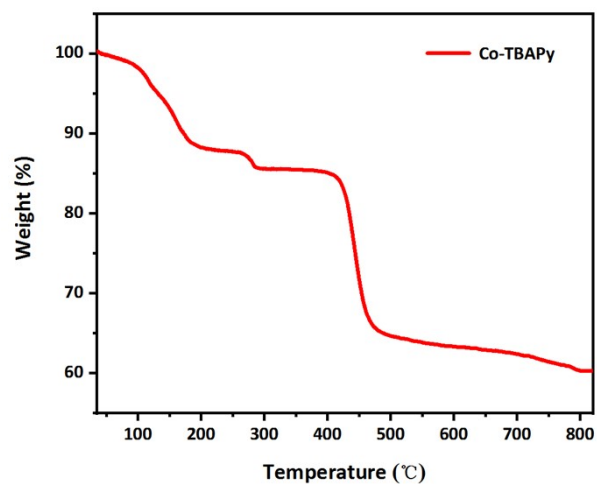


Figure S4. Thermogravimetric (TG) curve of Co-TBAPy.

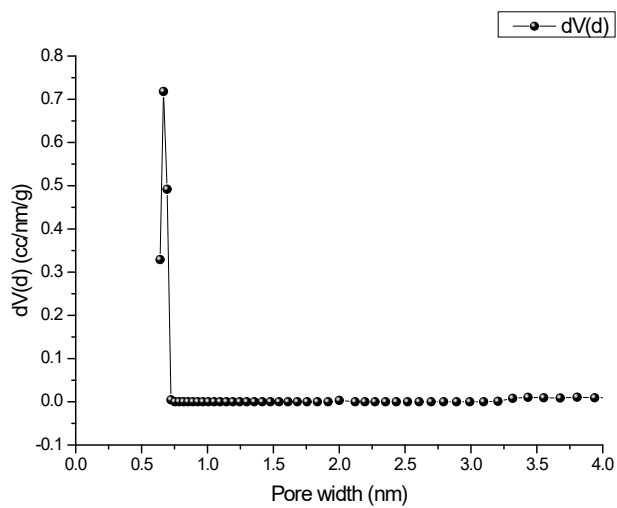


Figure S5. Pore size distribution curve of Co-TBAPy.

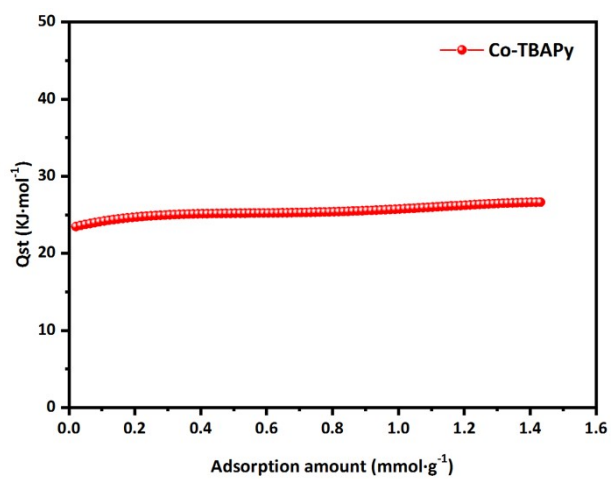


Figure S6. Adsorption enthalpy for carbon dioxide of Co-TBAPy.

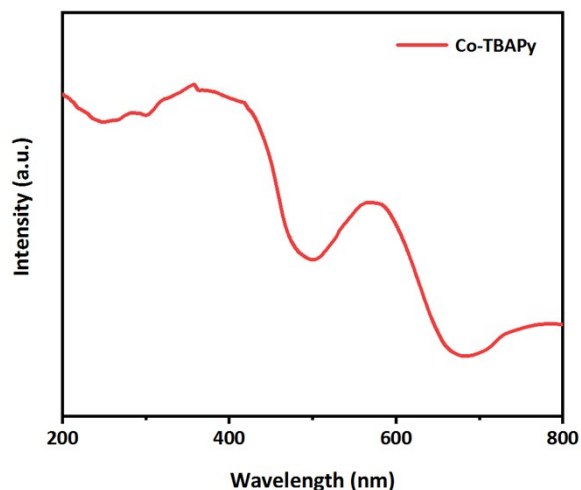


Figure S7. Ultraviolet-visible absorption (UV-Vis) spectrum of Co-TBAPy.

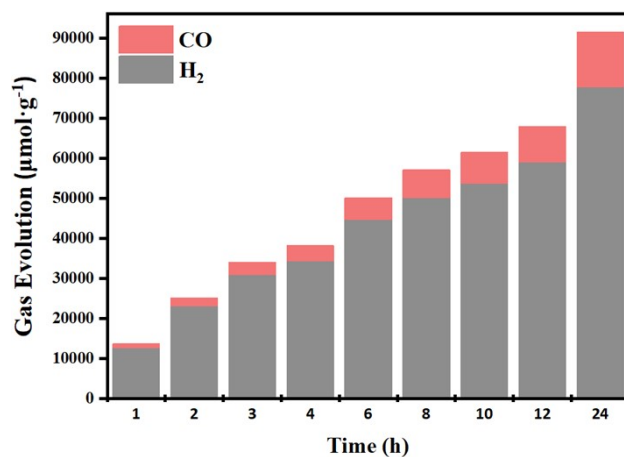


Figure S8. The H₂/CO ratio under the CO₂-saturated MeCN solution (5 mL) containing Co-TBAPy (5 μmol), [Ru(bpy)₃]Cl₂ (0.01 mmol), TEOA (1 mL) and H₂O (0.25 mL) at room temperature and irradiated by $\lambda > 420$ nm.

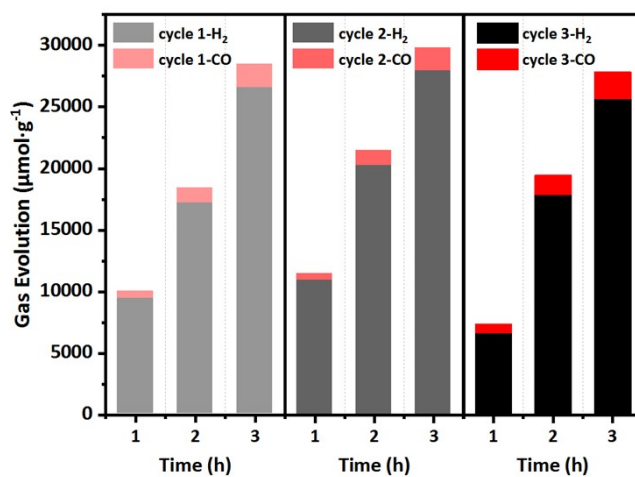


Figure S9. Amounts of CO and H₂ during three-run recycling experiments.

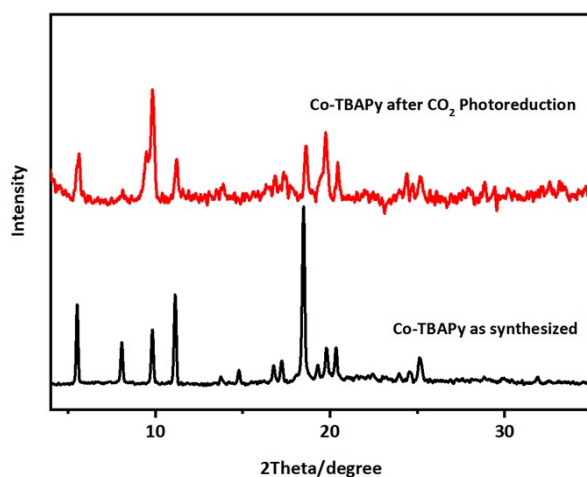


Figure S10. PXRD spectra of Co-TBAPy after photocatalytic CO₂ reduction compared with the as synthesized one.

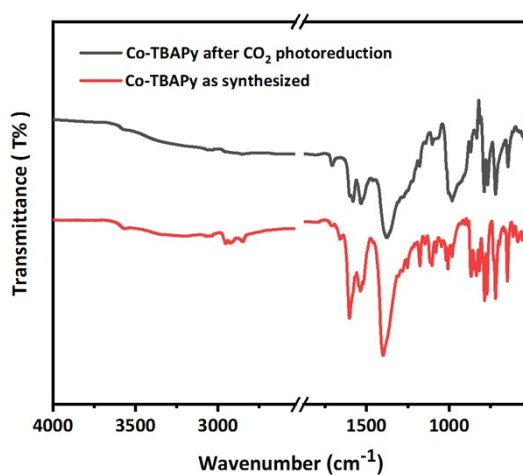


Figure S11. FT-IR spectra of Co-TBAPy after photocatalytic CO₂ reduction compared with the as synthesized one.

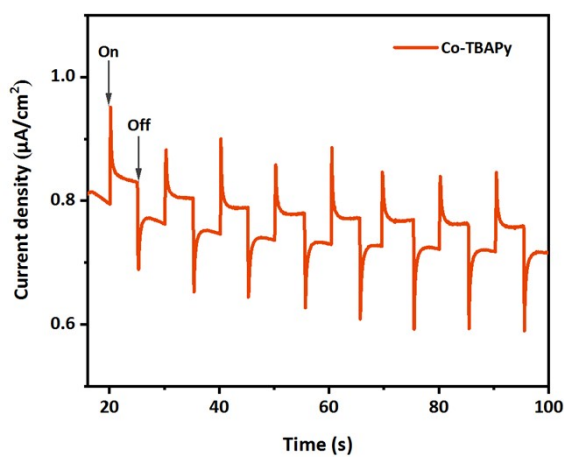


Figure S12. Photocurrent response curves of Co-TBAPy.

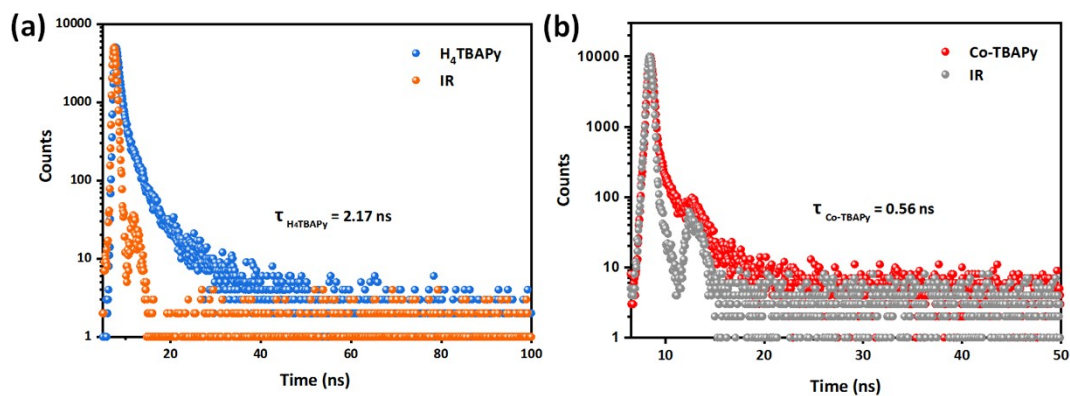


Figure S13. Time-resolved transient PL decay spectra of H₄TBAPy (a) and Co-TBAPy (b).

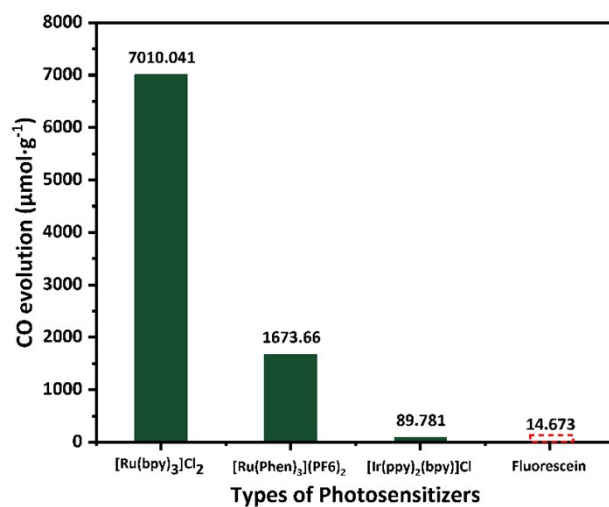


Figure S14. Amounts of CO detected using different types of photosensitizer.

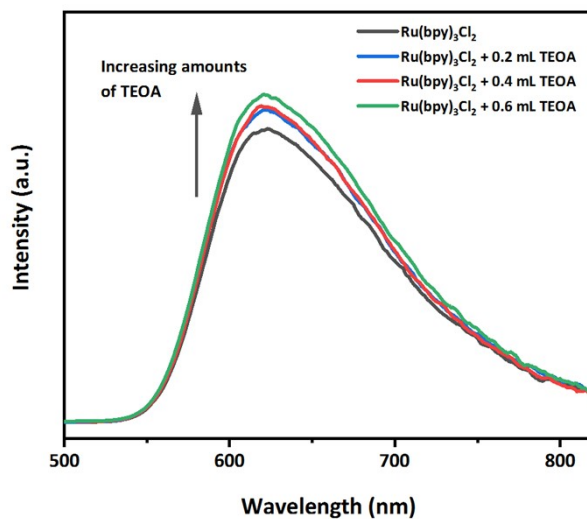


Figure S15. Steady state fluorescence spectra of [Ru(bpy)₃]Cl₂ upon the addition of increasing amounts of TEOA. ($\lambda_{\text{ex}} = 395 \text{ nm}$)

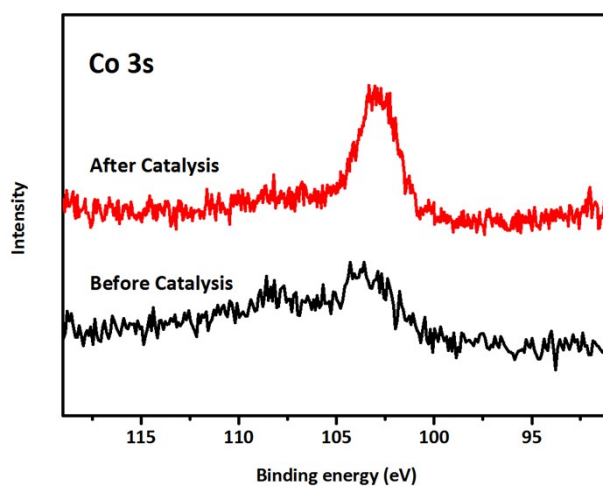


Figure S16. XPS spectrums of Co 3s orbit of Co-TBAPy before and after photocatalysis.

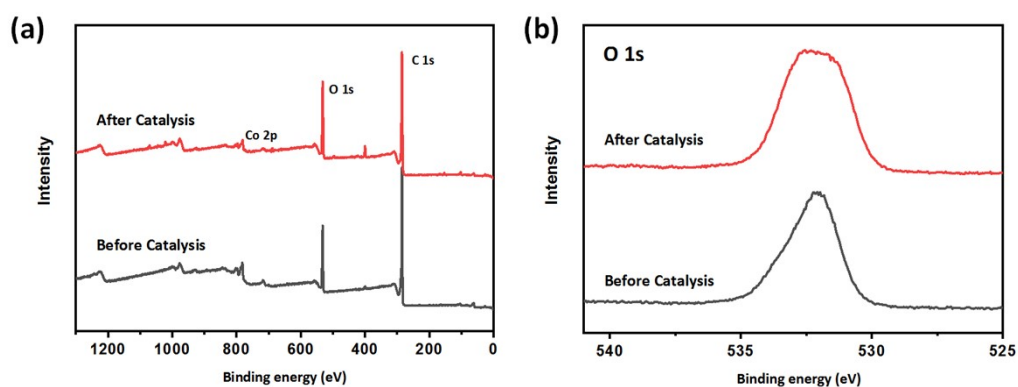


Figure S17. XPS spectrums of all elements (a) and O 1s orbit (b) of Co-TBAPy before and after photocatalysis.

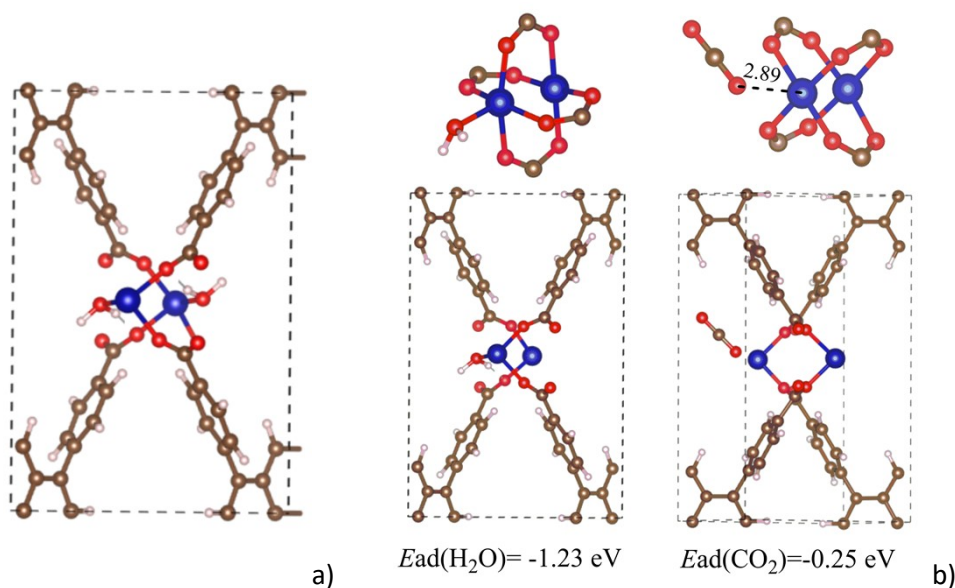


Figure S18. (a) The simulated configuration of Co-TBAPy. (b) The adsorption configuration of H₂O or CO₂ on Co-TBAPy. Color representation: brown, C; red, O; blue, Co; white, H.

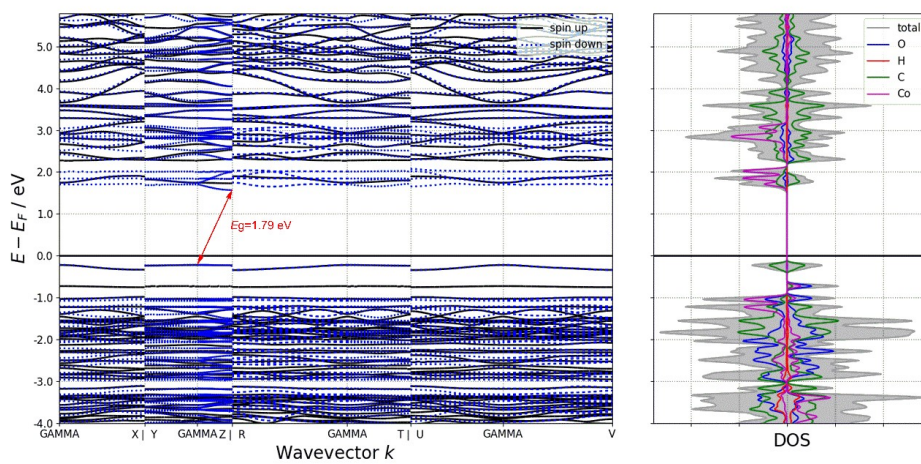


Figure S19. Band structure and density of states for Co-TBAPy.

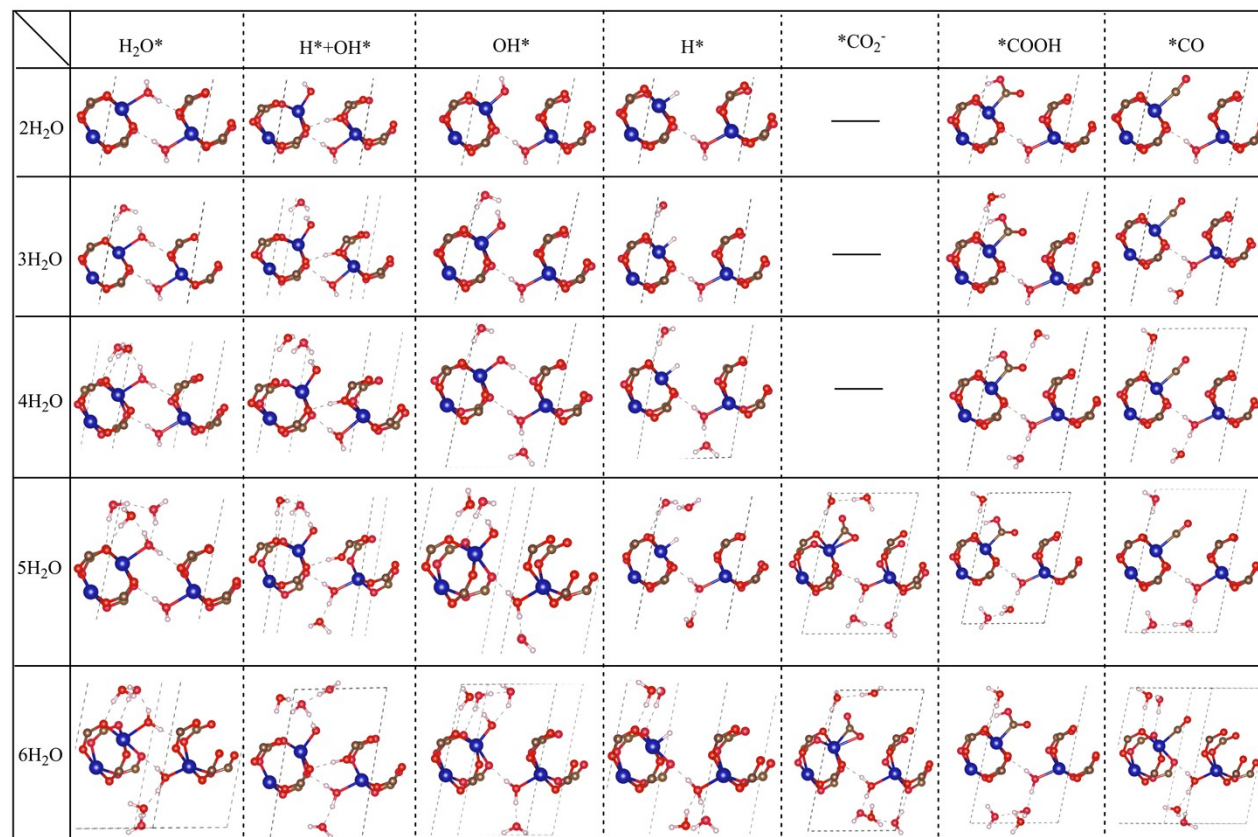


Figure S20. The intermediates along HER and CO_2RR pathways.

Table S1. Crystal data and structure refinement parameters for Co-TBAPy.

Co-TBAPy	
Empirical formula	C ₂₂ CoO ₅ H _{0.5}
Formula weight	403.65
Temperature/K	273.15
Crystal system	triclinic
Space group	<i>P</i> -1
<i>a</i> /Å	6.786(18)
<i>b</i> /Å	10.87(2)
<i>c</i> /Å	15.75(3)
α /°	87.31(6)
β /°	87.77(11)
γ /°	77.39(10)
Volume/Å ³	1132(4)
<i>Z</i>	2
ρ_{calc} (g/cm ³)	1.184
μ /mm ⁻¹	0.989
Reflections collected	1624
Independent reflections	1582
Goodness-of-fit on F ²	1.725
Final <i>R</i> indexes [<i>I</i> > 2 σ (<i>I</i>)]	<i>R</i> ₁ = 0.2009, <i>wR</i> ₂ = 0.4172
Final <i>R</i> indexes [all data]	<i>R</i> ₁ = 0.3024, <i>wR</i> ₂ = 0.4447

Table S2. The research of photocatalytic reaction conditions.^a

Entry	CO [μ mol]	H ₂ [μ mol]	TON ^b
1	37.13	52.06	17.84
2 ^c	n.d. ^d	n.d.	n.d.
3 ^e	1.10	5.06	1.23
4 ^f	n.d.	n.d.	n.d.
5 ^g	n.d.	n.d.	n.d.
6 ^h	0.02	2.24	0.45
7 ⁱ	1.72	32.84	6.91

a. Reaction conditions: [Ru(bpy)₃]Cl₂·6H₂O (0.01 mmol), Co-TBAPy (0.005 mmol, activated), acetonitrile (MeCN, 3.5 mL), H₂O (0.5 mL), TEOA (1 mL), CO₂ (1 atm), LED Lamp, λ > 420 nm, 25 °C, 10 h. b. Turnover number (mol amount of CO and H₂)/(mol amount of Co-TBAPy). c. Without Light. d. Not detectable. e. Without Co-TBAPy. f. Without [Ru(bpy)₃]Cl₂·6H₂O. g. Without the TEOA. h. Replacing the CO₂ with N₂. i. Low concentration of CO₂. (5% CO₂, 95% N₂).

Table S3. Comparison of the photocatalytic CO₂ reduction performance of analogous MOF-based catalysts, homogeneous complexes and semiconductor materials.

MOFs	Conditions							
	Quantity [μmol]	Light [nm]	Time [h]	CO [μmol]	H ₂ [μmol]	TON ^b	Syngas ratio (CO/H ₂)	Reference
Co-TBAPy	5	λ>420 nm	10	37.13	52.06	17.84	0.14-1.65	This work
Co ₆ -MOF	5	λ>420 nm	3	39.36	28.13	13.5	—	Ref. 1
Co-MOF-74	0.8	λ>420 nm	0.5	11.7	7.3	23.8	—	Ref. 2
Co-ZIF-9	4	λ>420 nm	2	20.8	3.3	6	—	Ref. 3
(Co/Ru) _{2,4} -UiO-67(bpydc)	1 mg	λ=450 nm, LED	16	4.52	9.12	—	0.33-0.53	Ref. 4
BIF-101	24.6	λ>420 nm	10	583	110	28.2	0.5-1	Ref. 5
[Co ₅ (btz) ₆ (NO ₃) ₄ (H ₂ O) ₄]	0.08	λ>420 nm	70	79.2	140.6	2748	0.06-0.5	Ref. 6
CoAl-LDH/MoS ₂	0.2-1.5 mg·mL ⁻¹	λ>400 nm	1	—	—	—	0.07-0.77	Ref. 7

Ref. 1: J. Zhao, Q. Wang, C. Sun, T. Zheng, L. Yan, M. Li, K. Shao, X. Wang and Z. Su, *J. Mater. Chem. A*, 2017, **5**, 12498.

Ref. 2: S. B. Wang, W. S. Yao, J. L. Lin, Z. X. Ding and X. C. Wang, *Angew. Chem. Int. Ed.*, 2014, **53**, 1034.

Ref. 3: S. B. Wang, J. L. Lin and X. C. Wang, *Phys. Chem. Chem. Phys.*, 2014, **16**, 14656.

Ref. 4: M. Liu, Y. F. Mu, S. Yao, S. Guo, X. W. Guo, Z. M. Zhang, T. B. Lu, *Appl. Catal. B: Environ.*, 2019, **245**, 496.

Ref. 5: Q. L. Hong, H. X. Zhang and J. Zhang, *J. Mater. Chem. A*, 2019, **7**, 17272.

Ref. 6: M. Sun, C. Wang, C. Y. Sun, M. Zhang, Z. M. Su. *J. Catal.*, 2020, **385**, 70.

Ref. 7: C. H. Qiu, X. J. Hao, L. Tan, X. Wang, W. J. Cao, J. Y. Liu, Y. F. Zhao and Y. F. Song. *Chem. Commun.*, 2020, **56**, 5354.